Electronic Supporting Information

Sub-micron spheres of an imine-based covalent organic framework: Supramolecular functionalization and water-dispersibility

David Rodríguez-San-Miguel,[a] Juan J. Corral-Pérez,[b] Eva Gil-González,[b] David Cuellas,[b] Jesús Arauzo,[b,c] Victor M. Monsalvo,[b] Verónica Carcelén,[,b] and Félix Zamora[*,a,d]*

[a]Departamento de Química Inorgánica, Universidad Autónoma de Madrid, Madrid, 28049, Spain.
[b]Campus de Palmas Altas, Calle Energía Solar nº1, Abengoa Research, Abengoa. Sevilla, 41014, Spain.
[c]Instituto Madrileño de Estudios Avanzados en Nanociencia (IMDEA Nanociencia), Cantoblanco, 28049 Madrid, Spain.
[d]University of Zaragoza, Thermochemical Process Group, Aaragon Institute of Engineering Research (I3A), I+D building, C/Mariano Esquillor s/n, E-50018 Zaragoza, Spain.

Section S1. Materials and Methods

All chemicals and solvents were purchased from commercial suppliers (Sigma-Aldrich, Carlo Erba Reagents and Acros Organics) and used without further purification. 1,3,5-tris(4-aminophenyl)benzene (TAPB) was synthesized according published procedures.[1,2]

Elemental analyses were obtained using LECO CHNS-932 elemental analyzer.

Attenuated Total Reflectance Infrared (ATR-IR) spectra were obtained in the 500-4000 cm^{-1} range using a Bruker Vertex 70 Fourier transform infrared (FTIR) spectrometer equipped with an ATR element. The signals are given in wavenumbers (cm^{-1}) and described as: very strong (vs), strong (s), medium (m), shoulder (sh), weak (w), very weak (vw) or broad (br).

High Resolution solid-state nuclear magnetic resonance (NMR) spectra were recorded at ambient pressure on a Bruker AV 400 WB spectrometer using a triple channel (BL4 X/Y/^{1}H) and Bruker magic angle-spinning (MAS) probe with 4 mm (outside diameter) zirconia rotors. The magic angle was adjusted by maximizing the number and amplitudes of the signals of the rotational echoes observed in the ^{79}Br MAS FID signal from KBr. Cross-polarization with MAS (CP-MAS) used to acquire ^{13}C data at 100.61 MHz. The ^{1}H ninety degree pulse widths were both 3.1 μs. The CP contact time varied from 3.5 ms. High power two-pulse phase modulation (TPPM) 1H decoupling was applied during data acquisition. The decoupling frequency corresponded to 80 kHz. The MAS sample spinning rate was 10 kHz. Recycle delays between scans were 4 s, depending upon the compound as determined by observing no apparent loss in the ^{13}C signal from one scan to the next. The ^{13}C chemical shifts are given relative to tetramethylsilane as zero ppm, calibrated using the methylene carbon signal of adamantane assigned to 29.5 ppm as secondary reference.

Samples of **sRT-COF-1** were characterized by X-Ray Diffraction (XRD) measurements performed using a SmartLab-Rigaku diffractometer equipped with a rotating anode (Cu Kα, $\lambda = 1.54180$ Å), a parabolic mirror to collimate the incident beam and a series of variable slits (placed before and after the sample).

Nitrogen adsorption and desorption measurements were done at 77K using an Autosorb-IQ-AG analyser (Quantachrome Instruments). **RT-COF-1** was activated at 100 ºC under vacuum for 12 h.

Dynamic Light Scattering (DLS) studies were carried out using a Vasco 1 particle size analyser of Cordouan Technologies.

Thermogravimetric Analyses of samples were run on a Thermobalance TGA Q-500 thermal gravimetric analyzer with samples held in a platinum pan under nitrogen atmosphere. A 10 K min^{-1} ramp rate was used. Sonication was carried out in an ultrasonication bath (Elma, 37 kHz and 380 W).

Scanning Electron Microscopy (SEM) images were carried out on a Hitachi S-4800 electron microscope.

Transmission Electron Microscopy (TEM) images were acquired in a FEI Tecnai F30 operated at 300 kV equipped with an EDS detector, a 2k x 2k Gatan digital camera with a spatial resolution of 0.19 nm. Ultramicrotomy, using Ultramicrotome Leica EM UC7, was applied to samples of **sRT-COF-1** in order to determine their internal structure. **sRT-COF-1** was embedded in an epoxy resin and dyed with uranyl acetate to enhance their contrast.

Atomic Force Microscope (AFM) techniques were use in dynamic mode using a Nanotec Electronica system operating at room temperature in ambient air conditions. The images were processed using WSxM (freely downloadable scanning probe microscopy software from www.nanotec.es). For AFM measurements, commercial Olympus Si/N cantilevers were used with a nominal force constant of 0.75 N/m. The surfaces used for AFM experiments were SiO_2 (300 nm thickness)/Si (IMS Company). In order to obtain reproducible results, very flat substrates were used with precisely controlled chemical functionalities, freshly prepared just before the chemical deposition. SiO_2 surfaces were sonicated for 15 min in acetone and 15 min in 2-propanol and then dried under an Argon flow.

AFM sample preparation were prepared by first dispersing 1 mg of **sRT-COF-1** in 1 mL of water, and sonicated with an ultrasonication bath (Elma, 37 kHz, 380 W) for 15 min. The resulting suspension was adsorbed on SiO_2 substrates by drop-casting deposition for 10 min at 20 ºC, and then dried under argon flow.

The kinetics precipitation was studied by UV-Vis (Agilent 8453) turbidimetry. Previously, pattern solutions of functionalized **sRT-COF-1** were required to find the calibration curves. This kinetic study started after functionalizing **sRT-COF-1** by sonication and leaving them statically at room temperature. The first measurement of **sRT-COF-1** concentration was carried out 1 h after the functionalization. 250 μL of the supernatant of the spheres suspension were picked up and diluted with 1 mL of water to measure the absorbance. The absorbance value was converted into concentration thanks to the calibration curves.

Preparations

*Synthesis of spherical **sRT-COF-1***: BTC (4.75 mg, 0.029 mmol) was dissolved in 1.5 mL of acetone. Separately, TAPB (10.25 mg, 0.029 mmol) was also dissolved in 1.5 mL of the same solvent. Both solutions were subsequently mixed and sonicated during 5 min. at 37 kHz. Then, 0.3 mL of acetic acid was added and the mixture stirred for 15 min. The yellow precipitated product was centrifuged at 15,000 rpm for 15 min. and washed with acetone (2 mL) twice and THF (2 mL). Finally, the solid was dried in an argon atmosphere at 170 ºC for 6 h to produce a pale yellow powder with a yield of *ca*. 60 %. Elemental analysis calculated for $C_{33}H_{21}N_3 \cdot H_2O$: C: 83.02 %; H: 4.82 %; N: 8.81 %. Found: C: 82.97 %; H: 4.88 %; N: 8.56 %. $C_{33}H_{21}N_3 \cdot H_2O$ contains 3.77 wt % of water (volatiles) in agreement with the TGA analysis (Figure S3).

Supramolecular functionalization: 1 mg of **sRT-COF-1** was dispersed in 3 mL of a 10% w/w surfactant/water solution by sonication for 30 minutes at 37 kHz and 380 W. The solid was isolated by centrifugation at 15,000 rpm for 15 min. and washed twice water, and then dried in an argon atmosphere at 170 ºC for 6 h.

Methylene blue adsorption test: 2.74 mg of **sRT-COF-1** are dispersed in 10 mL of water by sonication for 30 minutes at 37 kHz and 380 W. 257 µL of the resulting suspension are added to 2.743 mL of an aqueous solution of methylene blue ($3 \cdot 10^{-5}$ M). The mixture is stirred for 1 h. Then it is centrifuged at 14000 rpm for 5 min. The solid is washed thrice with 3 mL of water. The concentration of methylene blue in the supernatants was quantified by UV-Visible absorption spectroscopy.

Table S1. Summary of the experimental conditions tested for optimization of **sRT-COF-1** formation.

COF-1[a] (mg/mL)	**Acetic acid (%)**	**Acetone (%)**	**Other solvents**	**Sonication (min)** [b]	**Mean Diameter** [c] **(nm)**	**Dispersion** [c] **(nm)**
5	10	100	–	30	600	450-700
5	10	90	10% MeOH	30	555	500-708
5	10	66	34% MeOH	30	430	300-530
5	10	50	50% MeOH	60	340	150-420
5	10	66	34% *n*-Hexane	30	670	500-993

[a] This amount indicates the mg of **COF-1** expected after reaction of BTC and TAPB with 100 % yield. [b] 37 kHz. [c] Based on DLS measurements.

Section S2. Characterization of sRT-COF-1

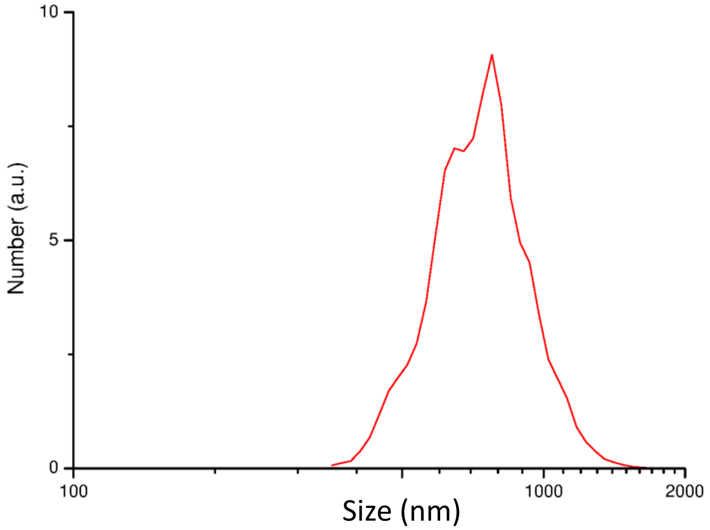

Figure S1. Dynamic Light Scattering of **sRT-COF-1** directly from the suspension obtained in its preparation.

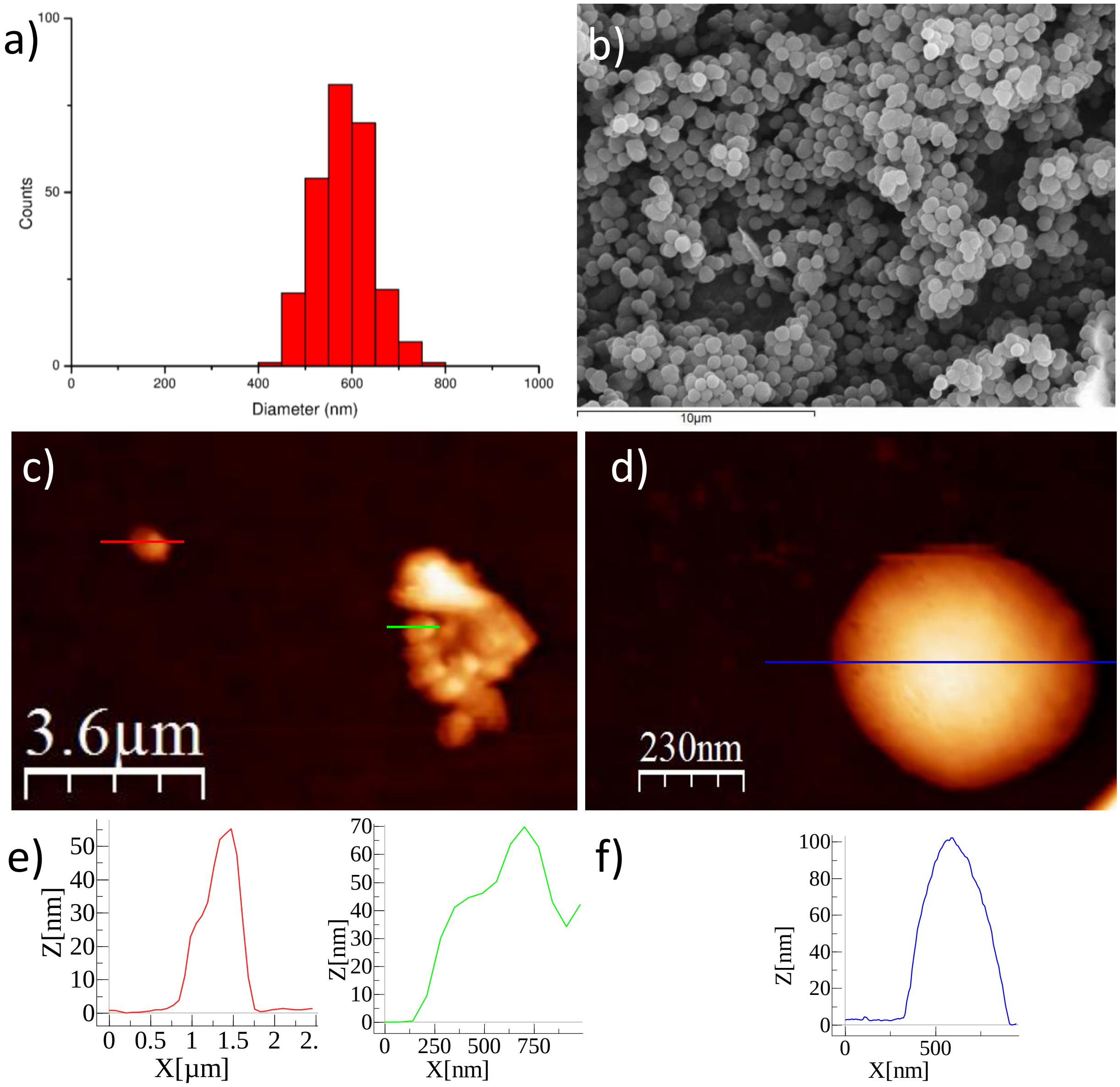

Figure S2. (a) Statistical analysis of the particles of **sRT-COF-1** measured in the SEM image of (b). AFM topographic image of diluted suspension of **sRT-COF-1** on SiO_2 (c) and a single **sRT-COF-1** sphere. Their heights profiles across the lines are provide in (e) and (f).

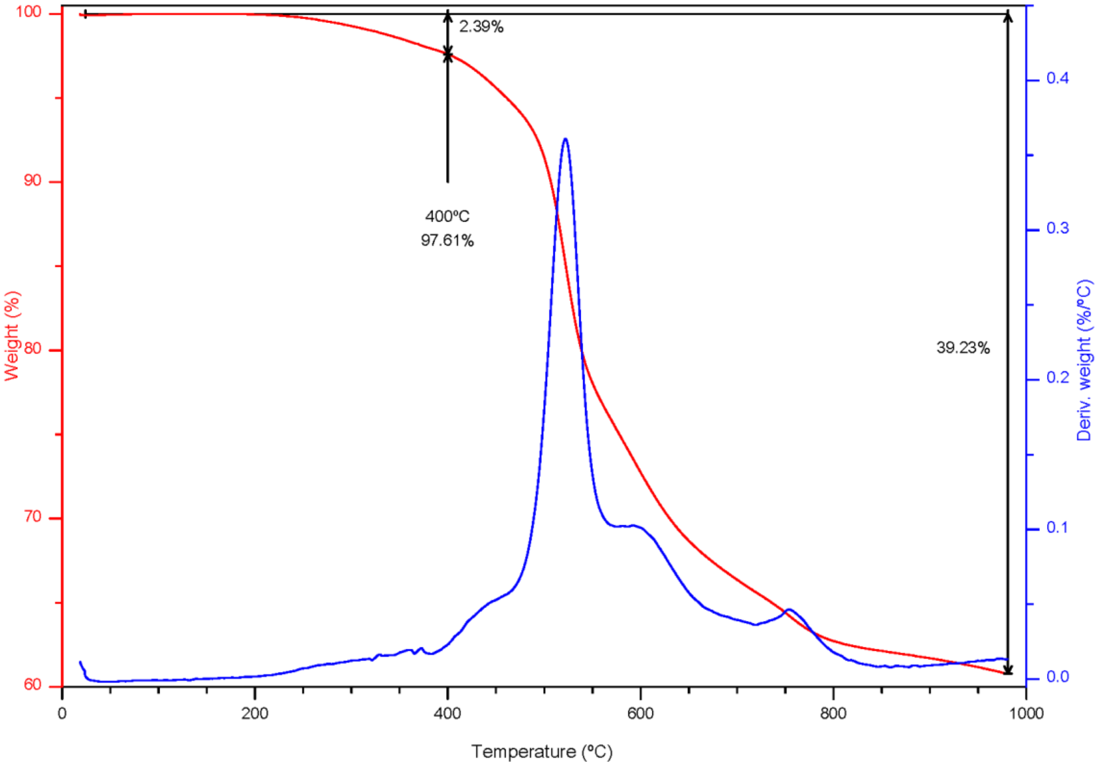

Figure S3. TGA profile of **sRT-COF-1** before the activation.

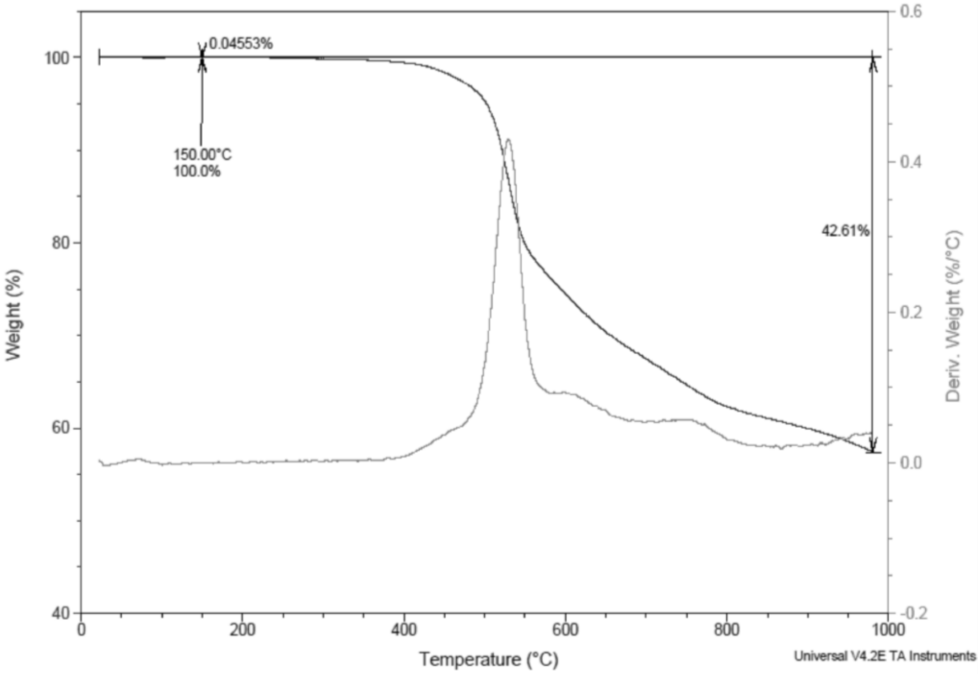

Figure S4. TGA profile of **sRT-COF-1** after the activation (100 ºC under vacuum overnight).

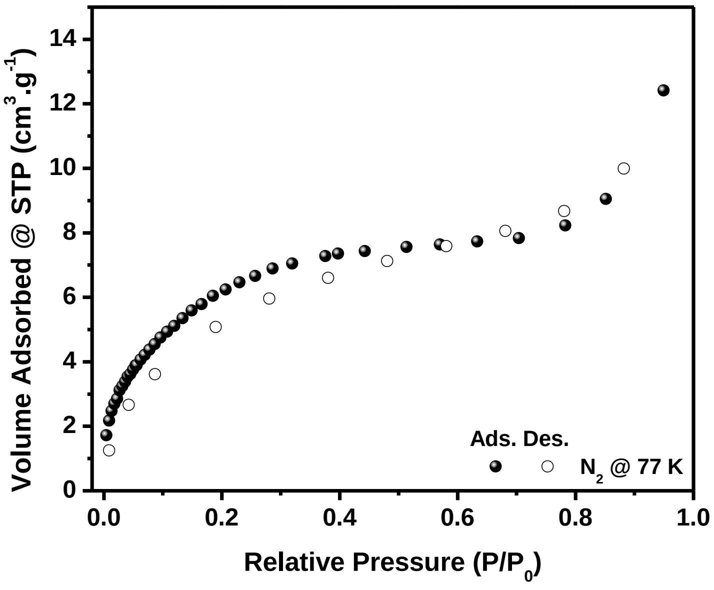

Figure S5. Nitrogen adsorption and desorption measurements for **sRT-COF-1** collected at 77 K.

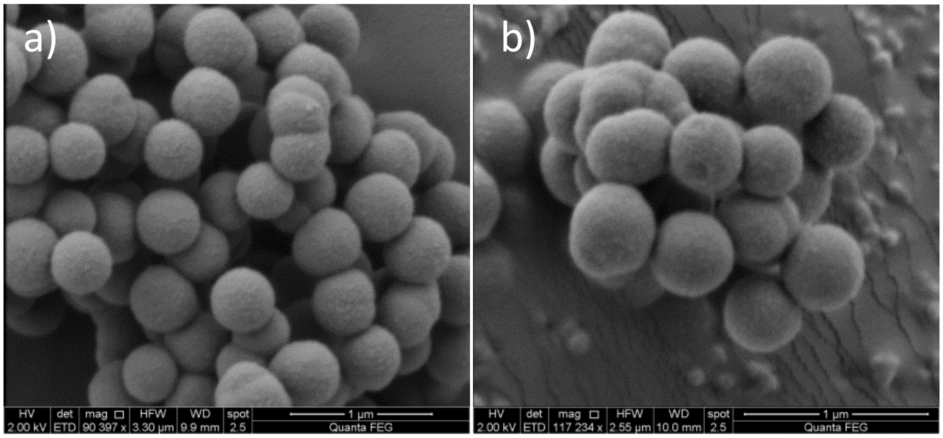

Figure S6. SEM images before (a) and after (b) nitrogen adsorption experiments.

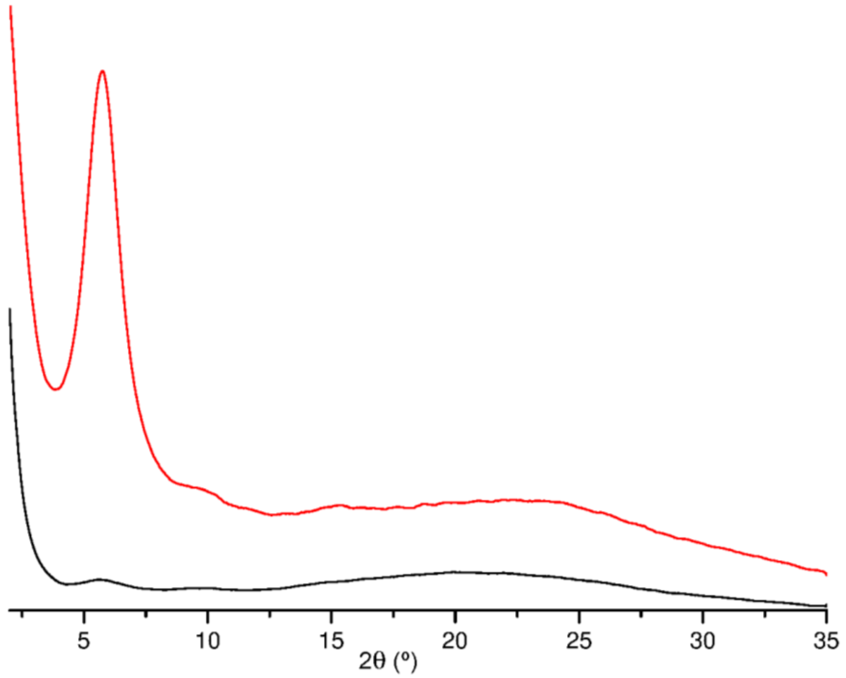

Figure S7. Powder X-Ray diffraction patterns of **sRT-COF-1** (black) and **RT-COF-1** (red).

Section S3. Spectroscopic Characterization

ATR-IR spectra

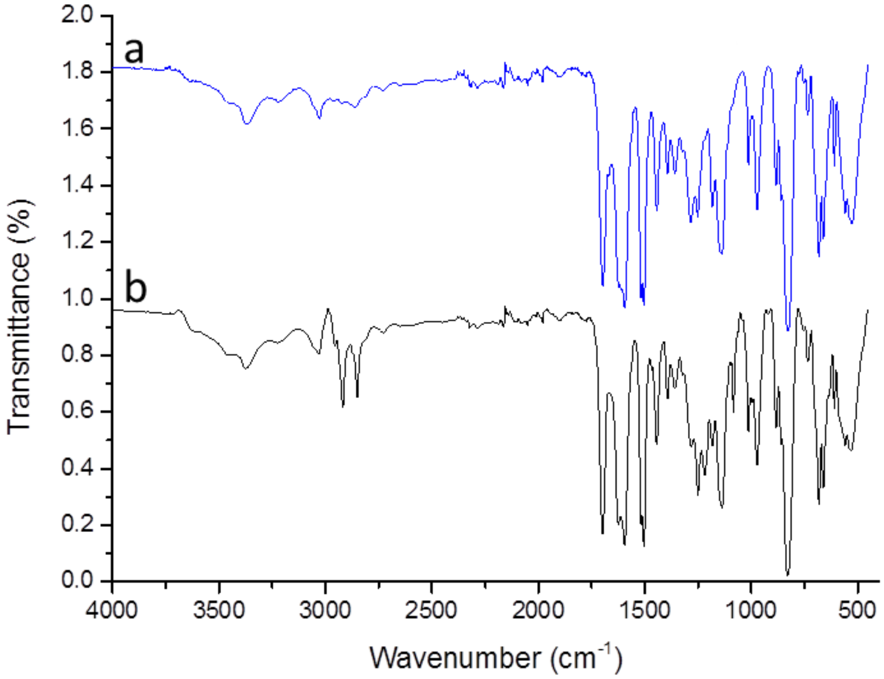

Figure S8. ATR-IR spectra of a) spherical **sRT-COF-1** and b) **sRT-COF-1** functionalized with SDS.

Table S2. Peaks assignment for ATR-IR spectrum of spherical **sRT-COF-1** without functionalization.

Peak (cm^{-1})	Assignment and notes
3372.3 (m)	N-H stretch from the unreacted NH_2 groups
3028.9 (w)	Aromatic C-H stretch
2863.1 (w)	C-H stretch from imine CH=N linkage
2286.1 (w)	Aromatic C-H bending overtones
2162.3 (w)	
2050.5 (w)	
1979.9 (w)	
1895.4 (w)	
1697.3 (s)	C=O stretch from the unreacted carbonyl groups
1621.6 (vs)	Imine C=N stretching
1594.3 (vs)	Aromatic ring stretching from phenyl rings
1517. 1 (s)	
1504. 8 (vs)	
1443.3 (s)	
1393.6 (m)	Aromatic ring bending
1358.7 (m)	Aromatic ring stretching from phenyl groups
1284.4 (m)	Single bond stretching from imine C-C=N-C- group
1251.5 (m)	Aromatic C-H in the plane ring vibrations
1182.6 (m)	
1139.1 (w)	
1012.9 (m)	Aromatic C-H in plane bending
972.4 (m)	Aromatic ring stretching
883.1 (w)	Aromatic C-H out of plane vibration
859.4 (w)	Aromatic ring stretching
827.0 (vw)	
762.4 (w)	C-H out of aromatic ring plane deformation from 1,3,5 trisubstituted benzenes
734.9 (s)	Methylenic C-H out of plane bending
681.9 (m)	Aromatic ring stretching

Table S3. Assignment for ATR-IR spectrum of spherical **sRT-COF-1** functionalized with SDS.

Peak (cm^{-1})	Assignation and notes
3373.5 (m)	N-H stretch from the unreacted NH_2 groups
3030.7 (w)	Aromatic C-H stretch
2955.8 (m)	Asymmetric CH_3 stretching, aliphatic CH_2
2918.4 (s)	
2850.5 (s)	
2728.9 (s)	
2323.7 (w)	Aromatic C-H bending overtones
2286.5 (w)	
2162.4 (w)	
2139.3 (w)	
2050.6 (w)	
1979.8 (w)	
1899.1 (w)	
1774.8 (w)	
1698.0 (s)	C=O stretch from the unreacted carbonyl groups
1623.0 (s)	Imine C=N stretching
1594.5 (vs)	Aromatic ring stretching from phenyl rings
1517.2 (s)	Aromatic ring stretching from phenyl rings
1504.6 (vs)	Aromatic ring stretching from phenyl rings
1443.9 (s)	Aromatic ring stretching from phenyl rings
1392.9 (m)	Aromatic ring bending
1358.5 (m)	Aromatic ring stretching from phenyl rings
1281.8 (m)	Single bond stretching from imine C-C=N-C- group
1250.6 (vs)	Aromatic C-H in the plane ring vibrations
1218.5 (s)	S=O stretching from SDS
1183.1 (m)	Aromatic C-H in the plane ring vibrations
1137.3 (w)	Aromatic C-H in the plane ring vibrations
1083.3 (m)	Symmetric SO_3 stretching from SDS
1013.1 (m)	Aromatic C-H in plane bending
972.6 (m)	Aromatic ring stretching
883.1 (w)	Aromatic ring stretching
859.2 (vs)	Aromatic ring stretching
829.3 (w)	C-H out of aromatic ring plane deformation from 1,3,5 trisubstitutedbenzenes
734.7 (s)	Methylenic C-H out of plane bending
681.7 (m)	Aromatic ring stretching

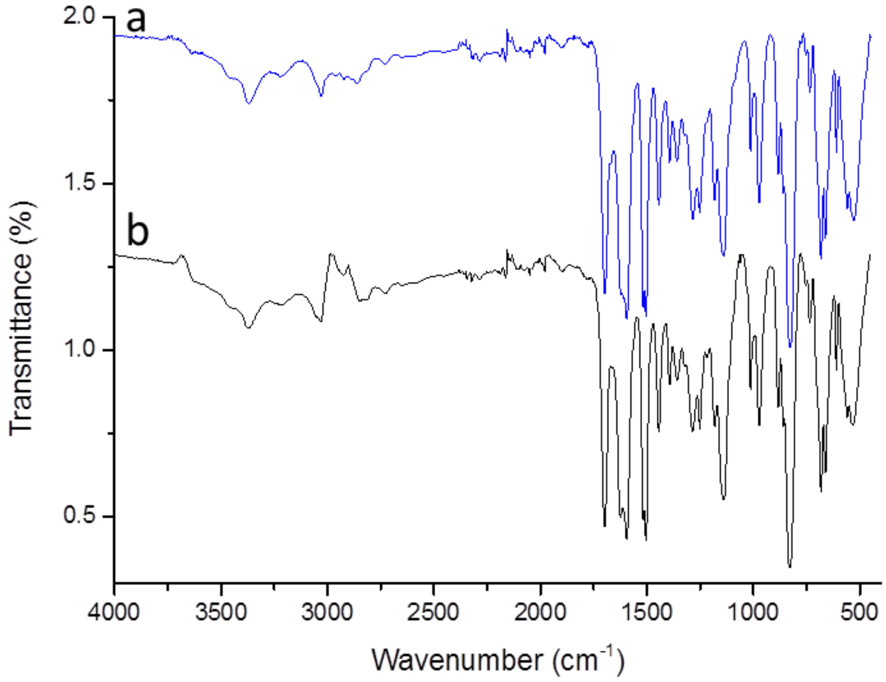

Figure S9. ATR-IR spectra of a) spherical **sRT-COF-1** and b) **sRT-COF-1** functionalized with SS.

Table S4. Assignment for ATR-IR spectrum of spherical **sRT-COF-1** functionalized with SS.

Peak (cm^{-1})	Assignation and notes
3372.9 (m)	N-H stretch from the unreacted NH_2 groups
3031.2 (w)	Aromatic C-H stretch
2927.4 (w)	Asymmetric CH_3 stretching, aliphatic CH_2
2848.9 (w)	
2728.5 (w)	
2323.3 (w)	Aromatic C-H bending overtones
2286.4 (w)	
2162.1 (w)	
2050.7 (w)	
1979.8 (w)	
1895.5 (w)	
1697.9 (s)	C=O stretch from the unreacted carbonyl groups
1623.6 (s)	Imine C=N stretching
1594.7 (vs)	Aromatic ring stretching from phenyl rings
1517.2 (s)	Aromatic ring stretching from phenyl rings
1504.5 (vs)	Aromatic ring stretching from phenyl rings
1443.7 (s)	Aromatic ring stretching from phenyl rings
1392.0 (m)	Aromatic ring bending
1357.7 (m)	Aromatic ring stretching from phenyl rings
1285.6 (m)	Single bond stretching from imine C-C=N-C- group
1251.3 (vs)	Aromatic C-H in the plane ring vibrations
1217.8 (s)	S=O stretching from SS
1182.2 (m)	Aromatic C-H in the plane ring vibrations
1137.8 (w)	Aromatic C-H in the plane ring vibrations
1012.9 (m)	Aromatic C-H in plane bending
972.39 (m)	Aromatic ring stretching
883.09 (w)	Aromatic ring stretching
859.26 (vs)	Aromatic ring stretching
829.25 (w)	C-H out of aromatic ring plane deformation from 1,3,5 trisubstituted benzenes
735.31 (s)	Methylenic C-H out of plane bending
681.7 (m)	Aromatic ring stretching

Solid-State ^{13}C CP-MAS Nuclear Magnetic Resonance Spectroscopy

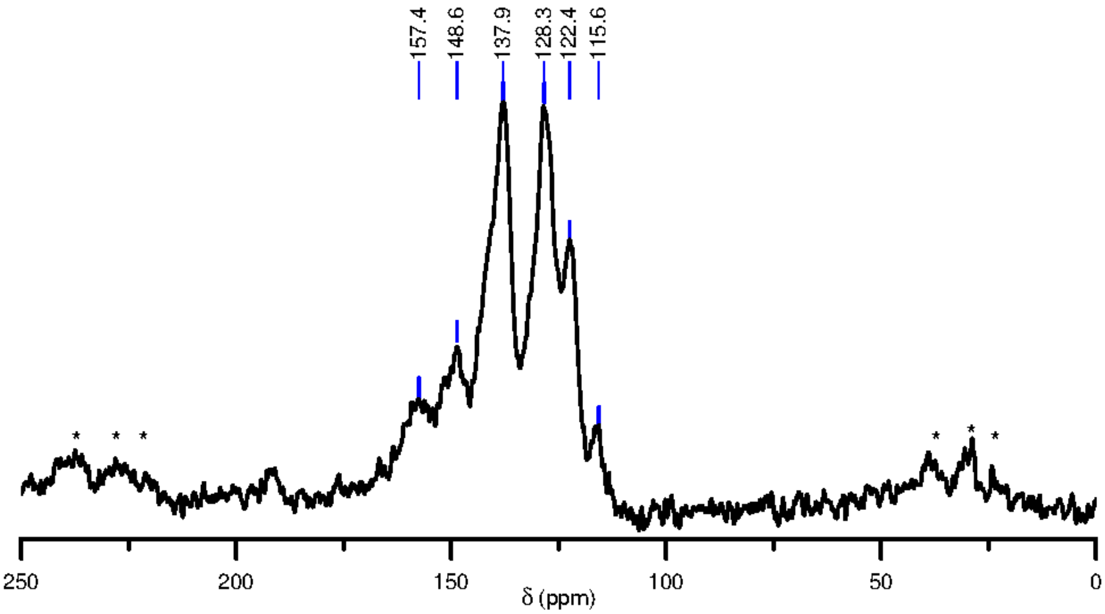

Figure S10. Solid-state ^{13}C CP-MAS spectrum of **sRT-COF-1**.

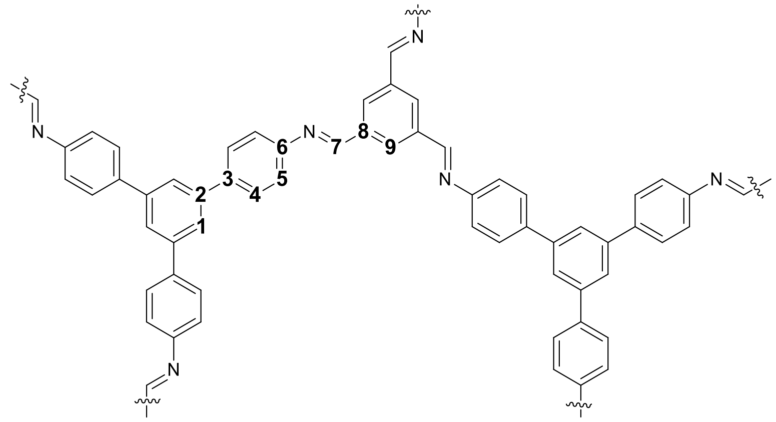

Signal (ppm)	Assignment	Comments
157.4	7	Imine carbon (alpha-imine, alpha-aromatic)
148.6	6	Aromatic carbon (alpha-imine)
137.9	2, 8, 9	Aromatic carbon (epsilon-imine, alpha-vinyl, beta-vinyl)
128.3	3, 4	Aromatic carbon (delta-imine, gamma-imine)
122.4	1	Aromatic carbon (zeta-imine)
115.6	5	Aromatic carbon (beta-aliphatic, beta-imine)

Section S4. Characterization of the process formation of sRT-COF-1.

A modified procedure was employed in order to decrease the reaction rate and allow the characterization of the intermediate stages of sphere formation. BTC (6 mg, 0.037 mmol) was dissolved in 2 mL of acetone. Separately, TAPB (13 mg, 0.037 mmol) was also dissolved in 2 mL of acetone. Both solutions were mixed and 0.1 mL of acetic acid was added.

This quantity of acetic acid was 4 times lower than the amount used in the standard procedure described in Section S1, which slows down the reaction considerably. Furthermore, the samples isolated for DLS and SEM were diluted in a 1/10 ratio, almost stopping the reaction.

These solutions were directly used in DLS measurements. SEM samples were prepared by casting a drop of the solution and blowing it with an argon flow after 10 seconds, in order to avoid the aggregation derived from drying.

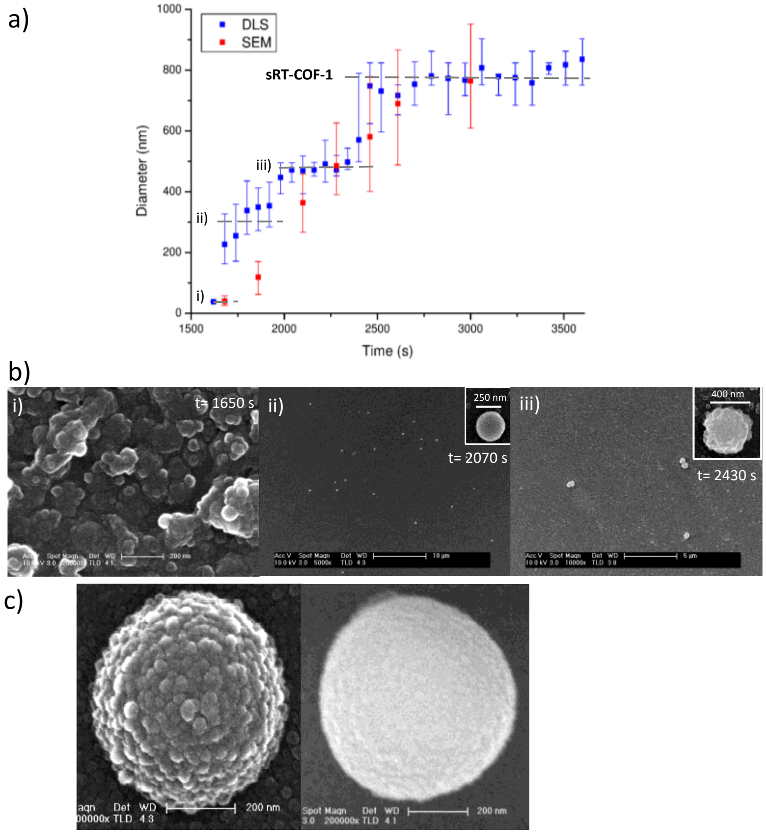

Figure S11. (a) Evolution of the particle size with the reaction time. Size estimated by both DLS and SEM. (b) Representative SEM micrographies of the nanoparticles isolated at the three different stages before formation of the **sRT-COF-1** spheres. (c) Evolution of the nanospheres with the reaction time showing a significant roughness reduction.

Section S5. Water Stability Studies.

As depicted in Figure S12, 1 mg of non- and functionalized spheres was dispersed in 3 mL of deionized water by sonication and was left statically at room temperature at time zero (t_0). After 384 h (t_1), non-functionalized spheres precipitated while functionalized ones were still dispersed in a stable suspension.

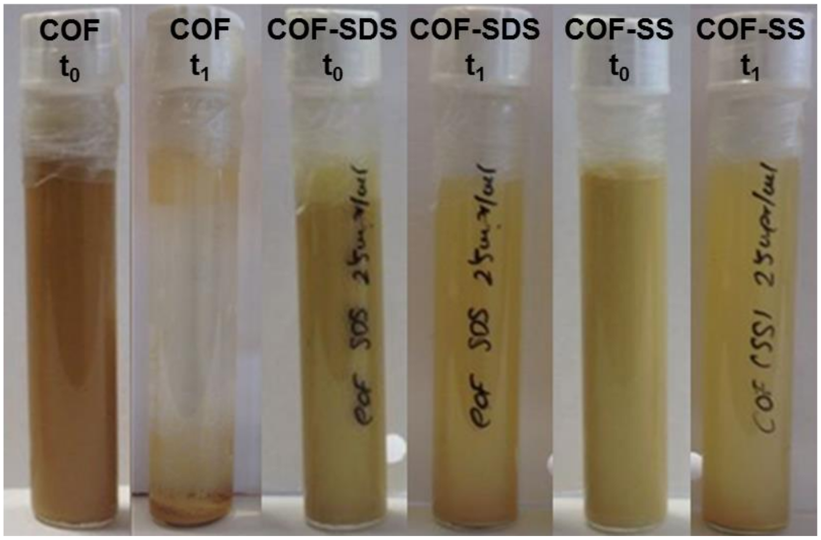

Figure S12. Aqueous solutions of non- and functionalized **sRT-COF-1** left statically at 25 ºC after sonication (t_0) and 384 h (t_1).

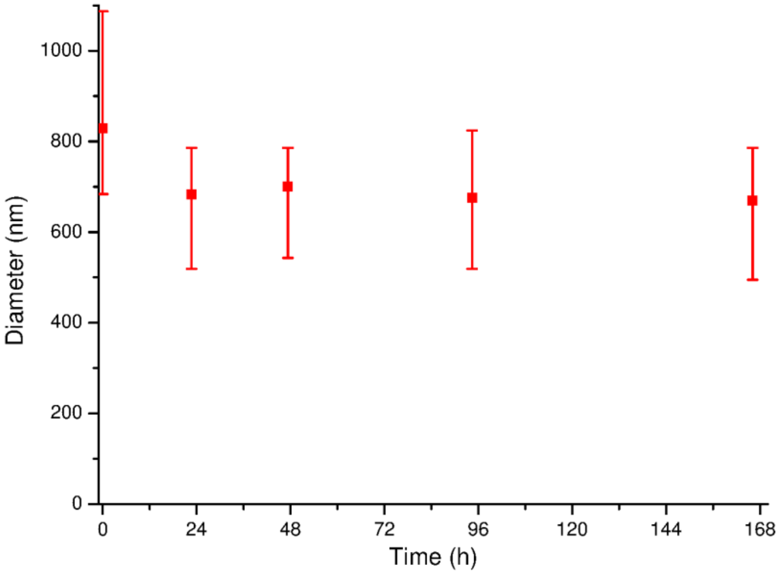

Figure S13. Evolution with time of the size (measured by DLS) of functionalized **sRT-COF-1**.

REFERENCES

(1) He, Y.; Bian, Z.; Kang, C.; Cheng, Y.; Gao, L. Novel C3-Symmetrical Triphenylbenzene-Based Organogelators with Different Linkers between Phenyl Ring and Alkyl Chain. *Tetrahedron* **2010**, *66* (19), 3553–3563.

(2) Rehab, A.; Akelah, A.; El-Gamal, M. M. Preparation of Novel, High-Modulus, Swollen- or Jungle- Gym-Type Polyimide Gels End-Crosslinked with 1,3,5-tris(4-Aminophenyl)benzene. *J. Polym. Sci. Part A Polym. Chem.* **2002**, *40*, 2501–2512.